

# Spitzer IRS-based Classification of Luminous $8\ \mu\text{m}$ Sources in the Large Magellanic Cloud

Stephen L. Thorndike<sup>1</sup>, Joel H. Kastner<sup>2</sup>, Catherine Buchanan<sup>2</sup>, Bruce J. Hrivnak<sup>3</sup>,  
Raghvendra Sahai<sup>4</sup>, & Michael Egan<sup>5</sup>

## ABSTRACT

To ascertain the nature of the brightest mid-infrared sources in the Large Magellanic Cloud (LMC), we have applied the Buchanan et al. (2006) *2MASS-MSX* color classification system, which is based on the results of *Spitzer Space Telescope* spectroscopy, to a mid-infrared ( $8\ \mu\text{m}$ ) flux-limited sample of 254 LMC objects for which 2MASS and MSX photometry is available. This sample is characterized by *MSX* A-band fluxes  $F_{8.3} \geq 150\ \text{mJy}$  and infrared ( $K - A$ ) colors in the range  $0.5 \lesssim K - A \lesssim 10$ . The results are as follows: 72 sources (28% of the sample) are most likely H II regions; 49 sources (19%) are identified as oxygen rich objects, where 42 (16%) of these are red supergiants and 7 (2%) are likely oxygen rich asymptotic giant branch (AGB) stars; 77 sources (30%) are identified as carbon-rich AGB stars; and 7 objects are found to be foreground Mira variables in the halo of the Milky Way. An additional 49 objects (19%) cannot be reliably classified based on their positions in 2MASS/MSX color-color and color-magnitude diagrams.

The large number of red supergiants compared to oxygen-rich AGB stars, and the large percentage of carbon stars among the sample, are consistent with the results of Buchanan et al. (2006) but now rest on a complete, flux-limited sample of LMC objects. The very large ratio of carbon-rich to oxygen-rich objects among the luminous and heavily dust-enshrouded AGB stars in our sample ( $\sim 10:1$ ) is consistent with the hypothesis that carbon stars form easily in lower metallicity

---

<sup>1</sup>Department of Physics & Astronomy, University of Rochester, Bausch & Lomb Hall, P.O. Box 270171, Rochester, NY 14627-0171 Email: slthorndike@astro.pas.rochester.edu

<sup>2</sup>Center for Imaging Science, Rochester Institute of Technology, 54 Lomb Memorial Drive, Rochester NY 14623. Email: clbsps,jhk@cis.rit.edu

<sup>3</sup>Dept. of Physics and Astronomy, Valparaiso University, Valparaiso, IN 46383

<sup>4</sup>NASA/JPL, 4800 Oak Grove Drive, Pasadena, CA 91109

<sup>5</sup>National Geospatial-Intelligence Agency, MS P-126, 12310 Sunrise Valley Dr., Reston, VA 20191-3449

environments. The number and color distributions of sources found for this sample can be extrapolated to other galaxies with metallicities similar to that of the LMC, so as to ascertain the nature of their populations of very luminous mid-infrared sources. As an initial step in this direction, we include a color-color diagram for the sample constructed from recently released *Spitzer* photometry obtained at 5.8, 8.0, and 24  $\mu\text{m}$ . The LMC’s populations of very luminous C-rich AGB stars and red supergiants appear as distinct clusters in this color-color diagram.

*Subject headings:* stars: AGB and post-AGB — Magellanic Clouds — infrared: stars — stars: mass loss — circumstellar matter

## 1. INTRODUCTION

To understand the chemical evolution of galaxies, we must observe evolved stars losing mass at large rates, as such stars dominate the rate of return of nucleosynthesis products into the interstellar medium. Due to its relative proximity, its low line of sight extinction, and its large stellar populations located at essentially uniform distance, the Large Magellanic Cloud (LMC) is an excellent target for such studies. Many optical surveys of the LMC have been conducted previously (Groenewegen 1999; Zaritsky et al. 1997; and refs. therein). However, these optical surveys do not yield information concerning the most rapidly mass-losing post-main sequence stars, as the optically-thick circumstellar dust envelopes associated with such stars absorb stellar photospheric emission and re-radiate this energy in the mid-to-far infrared. Hence, evolved stars with high mass loss rates must be studied in the infrared regime.

With the publication of the initial results of the recent *Spitzer Space Telescope* InfraRed Array Camera (IRAC) and Multiband Imaging Photometer for *Spitzer* (MIPS) imaging survey of the LMC (“Survey of the Agents of a Galaxy’s Evolution” [SAGE]; Meixner et al. 2006), broad-band infrared photometry at wavelengths of 3.6, 4.5, 5.8, 8.0 and 24  $\mu\text{m}$  is now available for over 30,000 mass-losing evolved stars in the LMC (Blum et al. 2006). For the most luminous of these LMC infrared sources, two predecessor infrared surveys — the Two Micron All-sky Survey (*2MASS*) and the LMC survey conducted by the Midcourse Space Experiment (*MSX*) — already have provided sensitive photometry in the wavelength range 1.2–8.3  $\mu\text{m}$ . Egan, Van Dyk & Price 2001 (hereafter EVP01) compared the A (8.3  $\mu\text{m}$ ) band magnitudes obtained from the *MSX* survey of the LMC with J (1.25  $\mu\text{m}$ ), H (1.65  $\mu\text{m}$ ), and K (2.17  $\mu\text{m}$ ) magnitudes obtained from *2MASS*. They identified 11 categories of stellar populations among the resulting sample of 1664 objects. EVP01 cross-checked their classifi-

cations of objects believed to reside in the LMC using spectral type data obtained from the SIMBAD database. However, only a small percentage of the most dust-obscured and, hence most luminous infrared sources in the LMC — i.e. those with  $8\ \mu\text{m}$  magnitudes  $m_A \lesssim 8$ , most of which EVP01 had classified as high mass loss oxygen-rich and carbon-rich asymptotic giant branch (AGB) stars, planetary nebulae (PNe), or H II regions — have spectral type classifications in SIMBAD. Most of these objects are also not readily classified on the basis of SAGE colors (Blum et al. 2006).

The use of IR spectra alleviates the ambiguity that results from assigning stellar classes based on IR photometry alone (Groenewegen et al. 1995; van Loon et al. 1998; Trams et al. 1999). The spectroscopic validation of infrared-color-based classification systems necessary to interpret the large volume of photometric data flowing out of SAGE and other *Spitzer* imaging surveys of Local Group galaxies is now possible using the *Spitzer* Infrared Spectrograph (*IRS*<sup>1</sup>). Several *Spitzer* IRS surveys of the LMC have been carried out, most of these aimed at its evolved star populations (e.g., Buchanan et al. 2006; Markwick-Kemper et al. 2005; Zijlstra et al. 2006; Groenewegen et al. 2007; Matsuura et al. 2006; Speck et al. 2006; Stanghellini et al. 2007). Buchanan et al. (2006), hereafter Paper I, conducted a spectroscopic study with *Spitzer* of a sample of the most luminous  $8\ \mu\text{m}$  sources in the LMC. These sources were chosen with the expectation that the sample would be dominated by highly evolved, rapidly mass-losing stars. The *IRS* spectra covered the range 5 to  $35\ \mu\text{m}$ , allowing the determination of evolved star envelope chemistries through identification of spectral signatures of C-rich and O-rich dust. The IR luminosities and evolutionary status of the objects were derived from the combined *2MASS*, *IRS* and (where available) IRAS spectral energy distributions.

Among their sample of  $\sim 60$  objects, gleaned from the lists of LMC evolved stars as classified by EVP01, Buchanan et al. (2006) identified 16 C-rich AGB stars, 4 O-rich AGB stars, 21 red supergiant (RSG) stars, and 2 OH/IR stars (one supergiant and one AGB star). They also found that this sample included 11 H II regions — presumably very young O or early B stars that are deeply embedded in their nascent, dusty, molecular clouds — as well as 2 B supergiants with peculiar mid-IR spectra suggestive of the presence of circumstellar disks (Kastner et al. 2006). In addition, four O-rich evolved stars were identified as foreground Mira variables located in the halo of the Milky Way. Buchanan et al. (2006) were thus able to establish a revised set of classifications of luminous  $8\ \mu\text{m}$  LMC sources on the basis of *IRS* spectra, IR spectral energy distributions, and IR luminosities of the objects in their sample. In particular, all of the objects EVP01 classified as PNe were reclassified as H II

---

<sup>1</sup>The IRS was a collaborative venture between Cornell University and Ball Aerospace Corporation funded by NASA through the Jet Propulsion Laboratory and Ames Research Center.

regions; most objects classified by EVP01 as OH/IR stars were reclassified as C-rich AGB stars; and objects classified by EVP01 as O-rich AGB stars were reclassified as either RSG or (in a handful of cases) foreground, mass-losing, O-rich AGB stars. Based on these Spitzer IRS-based results, we presented in Paper I a revised *2MASS/MSX* color-color and color-magnitude classification scheme for luminous  $8\ \mu\text{m}$  sources in the LMC.

The Paper I LMC *IRS* sample was selected to cover representative subsets of the types of luminous  $8\ \mu\text{m}$  sources in the LMC, but not their relative numbers. Therefore that study is not proportionally representative of the luminous mid-IR stellar populations of the LMC. Here, we revisit the entire sample of luminous  $8\ \mu\text{m}$  sources in the EVP01 lists to reclassify these objects according to the Paper I criteria. We thereby determine the distribution of infrared spectral types among a complete, flux-limited sample of LMC infrared sources.

## 2. THE SAMPLE

We began with all 1664 objects from the sample compiled by EVP01 that were identified in both the *MSX* and *2MASS* surveys. Initial selection included only those objects that had magnitudes measured for all four of the J, H, K, and A bands. In order to utilize Paper I magnitude criteria for identifying object types, we apply the same  $8.3\ \mu\text{m}$  magnitude limit,  $A \leq 6.5$  ( $F_{8.3} \geq 150\ \text{mJy}$ ). This eliminates  $\sim 70\%$  of the EVP01 sample. Objects that EVP01 classified as main sequence stars (“MS(V)”) were discarded from the sample on the grounds that these objects are neither evolved nor in the LMC. Those objects that EVP01 classified as MIII and A-K III and were bright J band *2MASS* sources were assumed to be giants residing in the halo of the Milky Way and were therefore also rejected. The objects *MSX* LMC 140, 421, 946, 1046, 1080, 1270, 1419, 1734, 1752, 1015, and 1049 were not designated as either MIII or A-K III stars by EVP01 but were classified as “star” or “Mstar” in the SIMBAD database. Given that the locations of these objects within *2MASS/MSX* color-color diagrams are indicative of photospheric rather than dust emission, these objects are also most likely foreground first-ascent red giants and were thus discarded.

The final sample considered here consists of 254 objects (Table 1). For this sample, Table 1 lists *MSX* name; SIMBAD designated name and spectral or object type; *2MASS* (J, H, and K) and *MSX* A magnitudes; IR types determined from *2MASS/MSX* colors by EVP01; IR types determined from the spectroscopy study presented in Paper I; and classifications we have assigned the objects in this paper, based on our color-color and color-magnitude criteria (§3). The rightmost column lists luminosities of the C-rich AGB and RSG objects, based on application of “bolometric corrections” developed in Paper I (§3.1). Table 2 contains a summary of the classifications of the Table 1 objects. The last two columns of Table 1 and

the summary in Table 2 thus reflect the results of the classification analysis carried out here (§3).

Figure 1 illustrates how the imposition of our MSX A-band minimum flux criterion effects the sample selection. In particular, note that the MSX flux limit restricts objects with RSG-like (i.e., relatively “blue”) spectral energy distributions to those that are very luminous in the near-infrared; such objects could be detected to much lower luminosities by both *2MASS* and *MSX* but would nonetheless be excluded from our sample. Conversely, many carbon stars and H II regions that meet our minimum  $8\ \mu\text{m}$  flux criteria are near the limits of detection by *2MASS*, such that slightly lower-luminosity examples of such objects would be missing from our sample. Similarly, certain evolved stars losing mass at very high rates — e.g., carbon stars and OH/IR stars with particularly optically thick circumstellar envelopes — may be excluded due to their non-detection by *2MASS*.

### 3. SPITZER IRS-BASED COLOR-COLOR AND COLOR-MAGNITUDE CLASSIFICATION OF LMC INFRARED SOURCES

The *2MASS* and *MSX* color-color diagrams constructed for our sample of objects are displayed in Fig. 2. We have overlaid the Paper I classification regions on these diagrams. Fig. 2 illustrates that the RSGs, O-rich AGB stars, and C-rich AGB stars form a sequence of increasing redness. There is a slight overlap between O-rich and C-rich AGB star classification regions that is poorly constrained due to the paucity of O-rich AGB stars in the Paper I sample. The galactic Mira variable (GMV) group occupies a subset of the RSG space and is therefore indistinguishable from RSGs based solely on these color-color diagrams. H II regions appear as a distinct group, due to their combination of blue  $J - K$  and  $H - K$  colors and very red  $K - A$  colors. Only a handful of objects in the Paper I study were found outside the regions indicated in Fig. 2. This “outlier” group consisted of two OH/IR stars found redward (in  $K - A$ ) of the C-rich AGB color-color “box”, and two B[e] supergiants with dusty circumstellar disks (Kastner et al. 2006) that lie between the RSG and H II region boxes.

In the present study, each object was classified primarily on the basis of its location in the *2MASS* and *MSX* color-color diagrams presented in Fig. 2. It is apparent from this Figure that most objects fall within the regions defined by the Paper I *2MASS/MSX* color criteria for identifying object types in the LMC. However, because we include all EVP01 objects satisfying the Paper I minimum *MSX*  $8\ \mu\text{m}$  flux criterion ( $F_{8.3} \geq 150\ \text{mJy}$ ), our enlarged sample encompasses color space that was not previously covered by the Spitzer IRS survey presented in Paper I. In certain cases we find no clear distinction between object

types, i.e., some objects lie on or near the dividing lines between RSG, O-rich AGB, and C-rich AGB zones in the color-color diagrams. A substantial fraction ( $\sim 25\%$ ) of sources also fall outside of the classification boxes established by Paper I. In particular, the color-color space occupied by candidate H II regions is larger than that sampled in the Paper I survey, as the Paper I H II region “box” was based on objects selected to have a fairly narrow range of  $2MASS$ - $MSX$  colors resembling those of PNe. Although it is possible some of the objects in our sample that lie outside the Paper I H II region box are PNe, there are various reasons to conclude the vast majority of objects in these regions of color-color space are H II regions (see Sec. 4.1).

As noted in Paper I,  $2MASS$  and  $MSX$  color-magnitude diagrams can help distinguish between object classes that are not clearly separable in color-color space. In Fig. 3, we present these color-magnitude diagrams for our sample. LMC RSGs and galactic Mira variables are clearly distinguished in this figure on the basis of near-infrared magnitude, due to the relative proximity of the latter group; while carbon stars and H II regions are readily separable on the basis of  $K - A$  and either  $J - K$  or  $H - K$  colors. Based on these results and the enlarged color space covered by our sample we have developed color-magnitude classification criteria that can be used to break certain degeneracies in the  $2MASS/MSX$  color-color diagrams (Table 3).

For objects that lie in the same, nonoverlapping classification regions in all color-color and color-magnitude diagrams, we ascribe high confidence to the classification assigned in Table 1. The classifications of objects that appear in a classification region on only one of the color-color plots are ascribed somewhat lower confidence (these tentative classifications are indicated by a colon in Table 1). There are also a small number of objects that are ambiguous in nature, i.e., that appear in different classification regions in different color-color and/or color-magnitude diagrams, that lie in overlapping regions on a given diagram, or whose  $2MASS/MSX$  color classifications conflict with their SIMBAD object types (footnote d in Table 1). With the exception of some objects tentatively classified as H II regions (§4.1), objects that do not lie in any classification region on any of the color-color diagrams are considered unclassifiable at present. For these objects, no classification is listed in Table 1.

The resulting, IRS-based classifications are listed in the next-to-last column of Table 1 and are summarized in Table 2. We display color-color diagrams illustrating the classification results in Fig. 4. A histogram of the number of objects in each class is displayed in Fig. 5. The classification results are discussed in detail in §4.

### 3.1. Estimates of infrared luminosities for RSGs and carbon stars

For LMC RSGs and luminous carbon stars, Paper I established empirical relationships between integrated infrared luminosity ( $L_{IR}$ ) and K-band flux density. In the case of carbon stars, the relationship depends on  $K - A$  color, while for RSGs the ratio of K-band flux to  $L_{IR}$  is roughly constant over the observed (relatively small) range of RSG  $K - A$  colors. We have applied these “bolometric corrections” to our sample; the results are listed in the last column of Table 1. The tabulated luminosities of the C-rich AGB and RSG stars have estimated uncertainties of  $\sim 30\%$  and  $15\%$ , respectively (Paper I), although these estimates do not take into account for the potential for large uncertainties due to source variability (particularly among the C-rich Miras in the sample).

## 4. DISCUSSION

### 4.1. H II Regions

We identify 72 sources (28% of the sample) as candidate H II regions. Of these, 21 fall within the Paper I H II region classification box in both of the *2MASS/MSX* color-color plots (Figure 2), and 27 fall in the H II region classification box on only one of the color-color plots. We classify another 18 objects as HII regions even though they lie “below” the H II region box; these objects are designated by an asterisk in Table 1. We classify these sources as H II regions because (a) it is clear that all of the objects in this region exhibit essentially the same near-IR to mid-IR colors indicative of very cool dust surrounding a relatively warm central region, and (b) all of the objects in this region of *2MASS-MSX* color-color space were classified as H II regions (as opposed to evolved stars or PNe) by EVP01. In addition to these (IRS- and IR-color-based) classifications and tentative classifications of objects as H II regions, we tentatively classify another 6 *MSX* sources as H II regions on the basis of their associated SIMBAD object types; these SIMBAD-based classifications are enclosed in square brackets in Table 1.

As noted in Paper I, many of the objects classified as H II regions are difficult to distinguish from planetary nebulae purely on the basis of *2MASS-MSX* colors. Indeed, of the 21 objects that fall within the H II region box on both of the color-color plots, all but 2 objects (*MSX* LMC 358 and 360) were previously classified as PNe by EVP01. However, all 11 of the EVP01 PN candidates selected for study in Paper I were revealed to be H II regions associated with young OB stars based on Spitzer IRS spectral features, extensive surrounding nebulosity apparent in optical/IR imaging, large mid-infrared source dimensions as inferred from IRS data, and/or exceedingly large luminosities ( $\gtrsim 10^5 L_{\odot}$ ).

With regard to this last (luminosity) criterion, 15 of the 17 candidate H II regions in Table 1 for which IRAS data are available have 25  $\mu\text{m}$  flux densities  $> 1.5$  Jy — similar to or, in many cases, larger than those of the H II regions studied in Paper I — and all of these display steeply rising SEDs in the IRAS data, indicative of luminosities  $\gtrsim 10^5 L_\odot$ . Furthermore, all but two of the objects that fell into only one of the H II region boxes in the color-color diagrams were previously classified by EVP01 as H II regions (the exceptions, *MSX* LMC 1296 and *MSX* LMC 938, were assigned PN classifications). Hence, we are reasonably confident of the accuracy of the classifications of the vast majority of the  $\sim 70$  H II regions in Table 1. Medium-resolution mid-infrared spectroscopy and close examination of archival imagery likely would establish unambiguously the natures of the objects we have thus far tentatively classified as H II regions.

#### 4.2. Red supergiants and oxygen-rich AGB stars

Oxygen-rich evolved stars represent the smallest group in our sample, with a total of 49 objects identified (19% of the Table 1 sample). The vast majority (42) of these are RSGs (17% of the sample), all but two of which fall in the RSG classification box in both color-color diagrams. Only seven candidate O-rich AGB stars appear to be present in our sample, four of which fall in the O-rich AGB classification box in both of the color-color diagrams. Another two stars here classified as RSGs on the basis of 2MASS/*MSX* colors, *MSX* LMC 813 (HV 12437) and *MSX* LMC 551, have inferred bolometric luminosities of  $\sim 4\text{--}5 \times 10^4 L_\odot$ , which is more consistent with upper AGB than RSG status. This suggests that the very small fraction of O-rich AGB stars in our sample — relative to the fraction of carbon stars of similar or smaller bolometric luminosity (§4.3) — may be in part a selection effect resulting from our minimum *MSX* A-band flux criterion and the “blue” mid-IR SEDs that are characteristic of O-rich AGB stars even at relatively high luminosity and mass loss rate. Spitzer IRS observations of fainter O-rich AGB candidates — i.e., objects with 8  $\mu\text{m}$  fluxes  $< 150$  mJy and 2MASS/*MSX* or SAGE colors consistent with those of the handful of high-luminosity, O-rich AGB stars identified in Paper I — are needed in order to better establish the relative frequency of O-rich vs. C-rich envelopes among the rapidly mass-losing AGB stars in the LMC.

Paper I established that four objects that reside within the O-rich AGB region (*MSX* LMC 412, 1150, 1677, and 1686) are in fact Mira variables located in the halo of the Milky Way. We have identified two and possibly three more GMVs in our sample, based primarily on their positions in the 2MASS-*MSX* color-magnitude diagrams (Fig. 3). One of these objects, *MSX* LMC 1048 (RT Men), was included in a sample of GMVs studied by



Jura & Kleinmann (1992) and was assigned a distance of 4.9 kpc. Another object, *MSX* LMC 362 (ZZ Men), was found by Wood & Bessell (1985) to have a radial velocity inconsistent with membership in the LMC. The third, *MSX* LMC 716, is designated as “M V” by SIMBAD but has an LMC stellar designation (“HV”) and in any case is far too red in the near- to mid-infrared to be a foreground main sequence M dwarf. It is possible that a few additional RSG candidates are in fact GMV stars, given the overlap in the regions of color-color space occupied by these classes (indeed, a half-dozen have ambiguous classifications; Table 1).

### 4.3. C-rich AGB stars

Carbon stars represent the single largest stellar population in our sample, with a total of 77 objects identified (30% of the sample). Of these, 54 are found to fall within the C-rich AGB box in both of the color-color diagrams, while 23 fall within this box in only one of the color-color diagrams. A majority of Table 1 objects classified as OH/IR stars by EVP01 are reclassified here as carbon stars as a consequence of the IRS survey results reported in Paper I. As C-rich with bluer  $K - A$  colors tend to overlap with O-rich AGB stars in *2MASS/MSX* color-color space (see Fig. 2), a small percentage of those objects lacking IRS spectra that are classified here as carbon stars may in fact be O-rich AGB stars.

Intriguingly, we find a handful of candidate carbon stars — *MSX* LMC 44 (IRAS 05112–6755), 83 (05091–6904), 888, 936 (05402–6956) and 1130 (04496–6958) — with inferred bolometric luminosities in the range  $L_{bol} \sim 2 \times 10^4 L_{\odot}$  to  $\sim 4 \times 10^4 L_{\odot}$  (IRAS 05112–6755 was included in an LMC carbon star sample studied with IRS by Matsuura et al. 2006). The brightest such object, *MSX* LMC 888, is particularly noteworthy, as its inferred luminosity of  $4.4 \times 10^4 L_{\odot}$  would place it very high on the AGB (the theoretical AGB limit being  $\sim 6 \times 10^4 L_{\odot}$ ; Iben & Renzini 1983). Recent models predict carbon star formation should be suppressed at such luminosities as a consequence of “hot bottom burning” (see review in Herwig 2005). Hence these candidate high-luminosity carbon stars, and *MSX* LMC 888 in particular, are particularly worthy of follow-up spectroscopy with the Spitzer IRS to confirm that they indeed display C-rich envelope chemistries. Furthermore, the very red colors of *MSX* LMC 888 and *MSX* LMC 635 (IRAS 05278–6942) — the latter a carbon star with  $L_{bol} \sim 3 \times 10^4 L_{\odot}$  (Groenewegen et al. 2007) and *2MASS/MSX* colors redder than those of the carbon stars surveyed in Paper I — indicates that more high- $L_{bol}$  carbon stars may lurk among the very red, unclassified objects in Table 1 (see below).

#### 4.4. Unclassified Objects

Out of our sample of 254 objects, 49 (19%) either do not fall into any of the color-color criteria, have infrared (*2MASS-MSX*) color-based classifications that are ambiguous, or have *2MASS-MSX* classifications that conflict with their SIMBAD (usually optical) classifications (Table 1). These objects — most of which are found above the H II region boxes and/or to the right of the O-AGB, C-AGB, RSG, and GMV boxes in *2MASS-MSX* color-color space (Fig. 4) — therefore remain unclassified. Four of the objects that cannot be classified solely on the basis of *2MASS-MSX* colors (*MSX* LMC 807, 890, 1182, and 1326) have been previously classified (Paper I; Kastner et al. 2006; and references therein) based on their IRS spectral properties and other previously known characteristics: *MSX* LMC 807 is an OH/IR (heavily dust-enshrouded, O-rich AGB) star, *MSX* LMC 1182 is an OH/IR supergiant, and *MSX* 890 and *MSX* 1326 are B[e] supergiants with circumstellar disks. Twenty of the objects we are unable to classify were also previously unclassified by EVP01.

Of the 88 objects in our sample that were classified as OH/IR stars by EVP01, 19 do not fall within any of the Paper I color-color classification boxes. Many of these are located just redward of the C-rich AGB box in  $K - A$  color (Fig. 4) and thus are most likely carbon stars with very high mass loss rates. These objects, like the candidate carbon stars with large luminosities, are worthy of spectroscopic investigation with the Spitzer IRS.

There also appears to be a small grouping of *MSX* sources in the region of color-color space where the B[e] supergiants *MSX* LMC 1326 and 890 are located (i.e., between the RSG and H II region classification boxes). Like *MSX* LMC 1326 and 890, several of these infrared sources (*MSX* LMC 134, 198, 646, and 1296) are associated with early-type emission line stars. A handful of additional *MSX* sources in other regions of *2MASS/MSX* color-color space (*MSX* LMC 262, 323, 583, 585, and 1438) also appear to be associated with early-type, emission-line stars, many of them supergiants (Table 1). Some or perhaps all of these *MSX* sources could indicate the presence of dusty circumstellar disks around the associated early-type stars (Kastner et al. 2006 and references therein).

### 5. SPITZER IRAC/MIPS COLORS OF THE SAMPLE OBJECTS

In Paper I, we demonstrated how the IRS spectral classifications of luminous LMC mid-IR sources could be used to classify sources on the basis of *Spitzer* IRAC/MIPS color-color diagrams. A color-color diagram constructed from IRAC 5.8 and 8.0  $\mu\text{m}$  and MIPS 24  $\mu\text{m}$  magnitudes appeared to offer particular promise in this regard. To explore this possibility,

we used the recently released SAGE IRAC and MIPS point source catalogs<sup>2</sup> to identify counterparts to Table 1 sources. Specifically, we selected all SAGE point sources with IRAC 8.0  $\mu\text{m}$  magnitudes  $\leq 6.5$  that have MIPS 24  $\mu\text{m}$  counterparts, and then cross-correlated their positions with the *2MASS* positions of the Table 1 sample, so as to identify those SAGE sources within  $7''$  (i.e., the approximate MIPS 24  $\mu\text{m}$  PSF FWHM) of a Table 1 object. This procedure resulted in a subsample of 172 SAGE counterparts to Table 1 sources. We note that most of the Table 1 objects missing from this subsample are candidate H II regions; these omissions most likely reflect the fact that IRAC is capable of resolving such sources and, hence, they were not included in the SAGE point source catalog. Source variability likely accounts for most of the remaining omissions of Table 1 sources from the SAGE subsample.

The  $[5.8] - [8.0]$  vs.  $[8.0] - [24]$  color-color diagram for the SAGE point source counterparts to Table 1 sources is displayed in Fig. 6. Carbon stars and RSGs appear as distinct clusters in this color-color diagram, confirming that the  $[5.8] - [8.0]$  vs.  $[8.0] - [24]$  color-color diagram is indeed an effective means to identify such objects among samples of luminous mid-IR point sources detected by IRAC/MIPS. Furthermore, those AGB stars whose O-rich nature has been firmly established via IRS spectroscopy also appear as a tight grouping. The overlap between O-rich AGB stars, very red C stars, H II regions, and the few unusual objects in Fig. 6, however, indicates this color-color diagram may be of more limited use in identifying the more extreme and/or exotic objects among samples of luminous mid-IR sources. Indeed, while Fig. 6 suggests potential classifications for many of the “unclassified” Table 1 objects — e.g., many lie “embedded” among the population of confirmed and candidate C stars, in IRAC/MIPS color-color space — IRS spectroscopy remains necessary to establish the natures of most of these unclassified sources.

## 6. SUMMARY AND CONCLUSIONS

To ascertain the nature of the most luminous mid-infrared sources in the LMC, we have applied the Buchanan et al. (2006) (Paper I) infrared (*2MASS-MSX*) color classification scheme — which is based on the results of Spitzer IRS spectroscopy of a representative sample of  $\sim 60$  objects selected from among the catalog of  $\sim 1650$  *2MASS/MSX* sources compiled by Egan et al. (2001) (EVP01) — to the entire EVP01 LMC sample satisfying the Paper I 8  $\mu\text{m}$  flux limit ( $F_{8.3} \geq 150$  mJy) and for which *2MASS* photometry is available. The latter criterion results in the exclusion of luminous 8  $\mu\text{m}$  sources with  $(K - A) \gtrsim 10$ .

---

<sup>2</sup>The SAGE point source catalogs are available via the GATOR interface to the NASA/IPAC Infrared Science Archive (<http://irsa.ipac.caltech.edu/applications/Gator/>).

After imposing these selection criteria and eliminating sources that are most likely foreground stars in the Milky Way, we are left with a sample of 254 *2MASS/MSX* sources. Among this sample, we classify 72 sources (28% of the sample) as confirmed or candidate H II regions; 49 (19%) as confirmed or candidate O-rich evolved stars, where 42 of these (17% of the sample) are RSGs and only 7 (3% of the sample) are candidate O-rich AGB stars; and 77 (30%) as confirmed or candidate C-rich AGB stars. We identify 7 sources as foreground (Milky Way) Mira variables. A total of 49 sources (19%) do not fall into any of the Paper I color-color criteria, have ambiguous infrared classifications, or have infrared classifications that conflict with their SIMBAD classifications; these objects therefore cannot be classified solely on the basis of *2MASS-MSX* colors, at present.

The  $\sim 6 : 1$  ratio of RSGs to O-rich AGB stars among our sample is consistent with that found in Paper I. We find the ratio of C-rich to O-rich objects is  $11 : 1$  among members of the luminous AGB star population in the LMC that satisfy the foregoing selection criteria, confirming that O-rich AGB stars are exceedingly rare among the most luminous  $8\ \mu\text{m}$  LMC objects with  $K - A \lesssim 10$ . These ratios remain somewhat uncertain, due to the likelihood that a fair fraction of the  $\sim 20\%$  of the sample that is presently unclassified are high-mass-loss-rate AGB stars. Nevertheless, the large number of C-rich AGB stars compared to O-rich AGB stars in our sample is consistent with the hypothesis that carbon stars form easily in low-metallicity environments, due to the relative ease of inverting the C/O ratio at the stellar surface (see review in Herwig (2005)). The relatively small ( $\sim 2 : 1$ ) ratio of AGB stars to RSGs among our sample is in keeping with the expectation that by selecting the most luminous  $8\ \mu\text{m}$  sources among the population of highly evolved stars in the LMC, we are sampling the intermediate-to-high range of initial stellar mass.

We applied “bolometric corrections,” established empirically in Paper I, to estimate the integrated infrared luminosities of carbon stars and RSGs based on their K-band magnitudes. Because our sample includes all luminous  $8\ \mu\text{m}$  LMC sources with *2MASS* counterparts, these estimates directly yield the peak luminosities reached by relatively “blue” RSGs (with  $K - A \lesssim 3$ ) and those LMC carbon stars which have  $K - A \lesssim 6$ . The most luminous such RSG in the LMC therefore appears to be *MSX* LMC 43 (HV 888), with an estimated luminosity of  $1.9 \times 10^5 L_\odot$ . This luminosity falls well short of that of the OH/IR supergiant *MSX* LMC 1182 (IRAS 04533–6933, with  $L_\star \sim 5 \times 10^5 L_\odot$ ; Paper I); it remains possible that other very luminous and highly obscured red supergiants lurk among the unclassified objects in our sample. Meanwhile, the most luminous carbon stars in our sample rise very high on the AGB; the C-rich AGB candidate *MSX* LMC 888 approaches theoretical expectations for the peak luminosities of carbon stars (Herwig 2005).

Given similar selection criteria, the distribution of luminous  $8\ \mu\text{m}$  sources established

here for the LMC (Table 2; Fig. 5) can be extrapolated to other galaxies with similar metallicities, so as to ascertain the nature of their populations of very luminous mid-infrared sources. Furthermore, we have demonstrated that a  $[5.8] - [8.0]$  vs.  $[8.0] - [24]$  color-color diagram constructed from IRAC/MIPS photometry provides a particularly effective means to identify carbon stars and red supergiants among samples of luminous mid-IR point sources detected via *Spitzer* imaging of the Milky Way and external galaxies.

Further *Spitzer* IRS spectroscopic observations of the sample of luminous  $8\ \mu\text{m}$  LMC sources presented here would establish the nature of the  $\sim 50$  (mostly very red) objects that we are unable to classify on the basis of *2MASS-MSX* colors, would confirm whether the  $\sim 30$  objects we have tentatively classified as H II regions are in fact such objects, and would likely turn up additional O/B stars with dusty circumstellar disks. In addition *Spitzer* spectroscopic observations of objects with *2MASS/MSX* colors similar to those of the few O-rich AGB stars in Table 1, but with smaller  $8\ \mu\text{m}$  luminosities, are required to establish whether, and to what degree, our selection criteria bias our finding of a very large ratio of C-rich to O-rich AGB stars in the LMC. Such observations would also establish whether the distinct clusters of C-rich AGB stars and RGSs that appear in the IRAC/MIPS color-color diagram constructed for luminous  $8\ \mu\text{m}$  LMC sources (Fig. 6) persist to lower luminosity.

The authors thank Bill Forrest for his incisive comments on this manuscript. Support for this research was provided by JPL/Caltech *Spitzer* Space Telescope General Observer grant NMO710076/1265276 to R.I.T.

*Facilities: Spitzer*

## REFERENCES

- Blum, R.D., Mould, J.R., Olsen, K.D., et al. 2006, *AJ*, 132, 2034
- Buchanan, C. L., Kastner, J. H., Forrest, W. J., Hrivnak, B. J., Sahai, R., Egan, M., Frank, A., & Barnbaum, C. 2006, *AJ*, 132, 1890 (Paper I)
- Egan, M. P., Van Dyk, S. D., & Price, S. D. 2001, *AJ*, 122, 1844 (EVP01)
- Groenewegen, M. A. T., Smith, C. H., Wood, P. R., Omont, A., & Fujiyoshi, T. 1995, *AJ*, 119, 449
- Groenewegen, M. A. T. 1999, *IAU Symp. 191: Asymptotic Giant Branch Stars* (San Francisco: ASP), 191, 535

- Groenewegen, M. A. T., 2007, MNRAS, in press
- Herwig, F. 2005, ARA&A, 43, 435
- Iben, I. Jr., Renzini, A. 1983, Annu. Rev. A&A, 21, 271
- Jura, M., & Kleinmann, S. G. 1992, ApJS, 79, 105
- Kastner, J. H., Buchanan, C. L., Sargent, B., & Forrest, W. J. 2006, ApJ, 638, L29 S. D., & Walker, H. J. 2002, ApJS, 140, 389
- Markwick-Kemper, C. et al. 2005, IAU Symp. 231, p. 134
- Matsuura, M., Wood, P. R., Sloan, G. C., et al. 2006, MNRAS, 371, 415
- Meixner, M., Gordon, K. D., Indebetouw, R., et al. 2006, AJ, 132, 2268
- Speck, A., et al. 2006, ApJ, 650, 892
- Stanghellini, L. et al. 2007, in “Planetary Nebulae in Our Galaxy and Beyond,” Proc. IAU Symp. 234, eds. M.J. Barlow & R.H. Mendez (Cambridge U. Press), p. 313
- Trams, N. R., van Loon, J. Th., Waters, L. B. F. M., Zijlstra, A. A., Loup, C., Whitelock, P. A., Groenewegen, M. A. T., Blommaert, J. A. D. L., Siebenmorgen, R., Heske, A., & Feast, M. W. 1999, A&A, 346, 843
- van Loon, J. T., Zijlstra, A. A., Whitelock, P. A., Te Lintel Hekkert, P., Chapman, J. M., Loup, C., Groenewegen, M. A. T., Waters, L. B. F. M., & Trams, N. R. 1998, AJ, 169, 329
- Wood, P. R., & Bessell, M. S. 1985, PASP, 97, 681
- Zaritsky, D., Harris, J., & Thompson, I. 1997, AJ, 114, 1002
- Zijlstra, A. et al. 2006, MNRAS 370, 1961

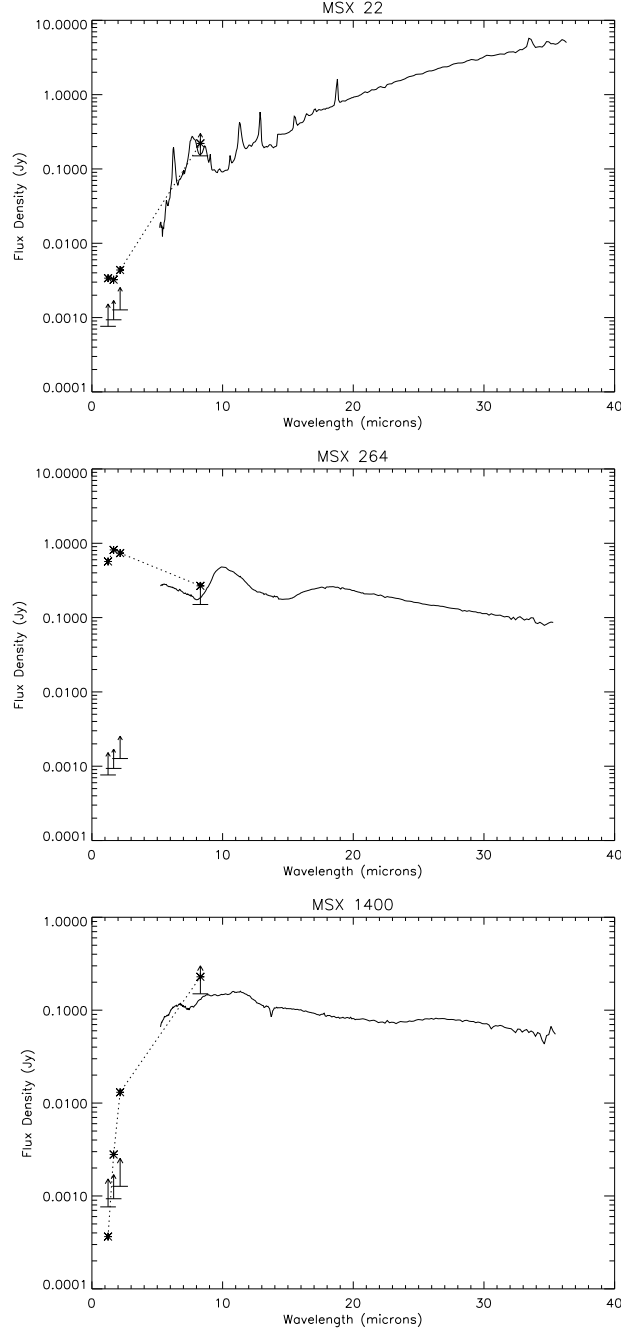


Fig. 1.— *2MASS*–*MSX*–*IRS* spectral energy distributions of a representative H II region (*MSX* 22), O-rich RSG (*MSX* 264), and C-rich AGB star (*MSX* 1400), compared with *2MASS* sensitivity limits and the *MSX* A-band magnitude limit imposed both in Paper I and in the present study (bars with arrows). Spectra are indicated as solid lines, and *2MASS*/*MSX* photometry as asterisks.

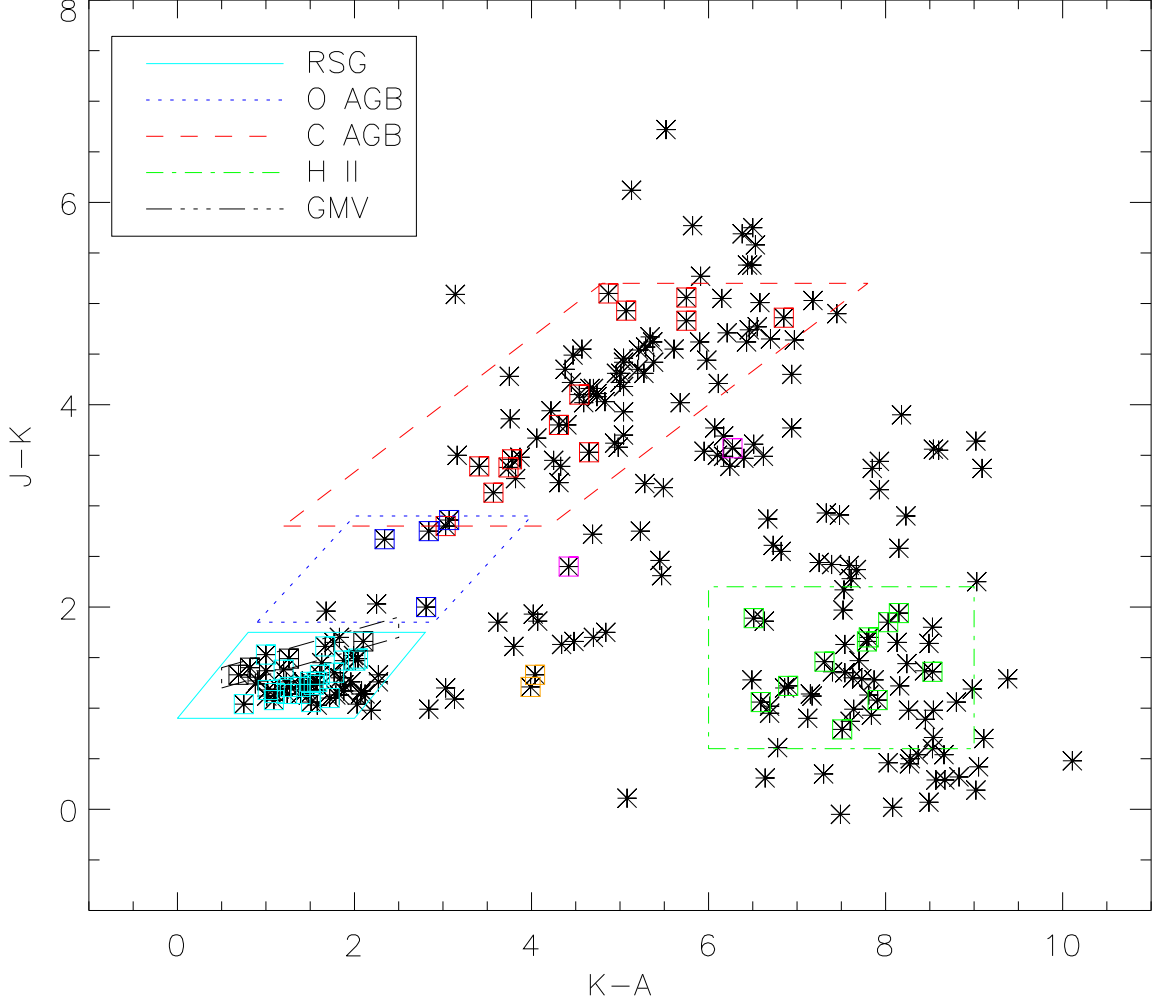


Fig. 2.— (a) *2MASS/MSX* color-color diagram displaying  $J - K$  vs.  $K - A$  colors for the Table 1 sample. The boxes indicate the Paper I Spitzer IRS-based infrared color criteria for classification of IR-luminous LMC objects. The small squares enclose points corresponding to objects with IRS spectra obtained in the Paper I survey. The colors of the boxes and squares correspond to Paper I infrared class, as indicated in the figure legend. Magenta and orange squares indicate the positions of two OH/IR stars and two supergiant B[e] stars with dusty disks, respectively.



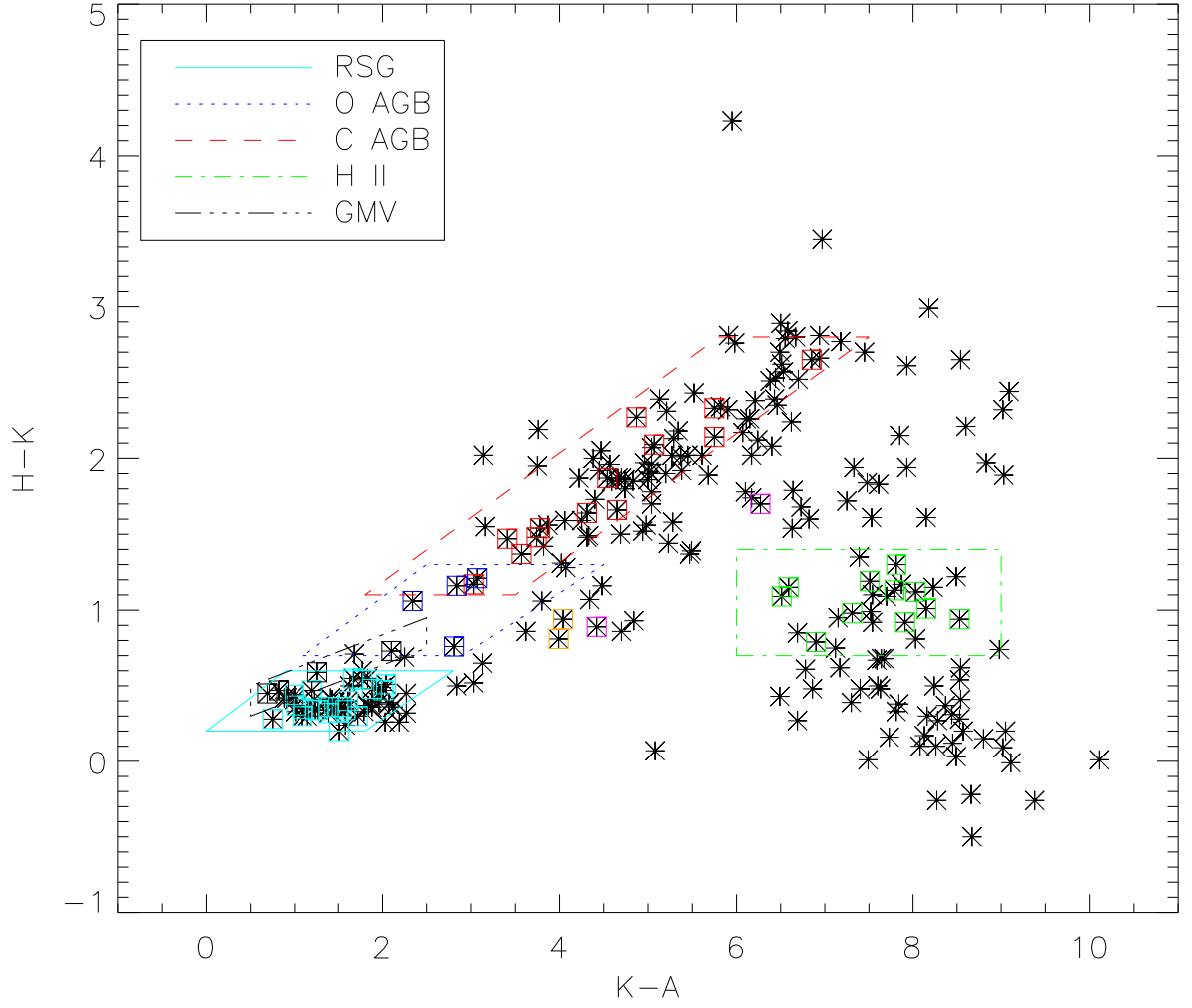


Fig. 2.— (b) As in Figure 2 (a), but for  $H-K$  vs.  $K-A$  colors.

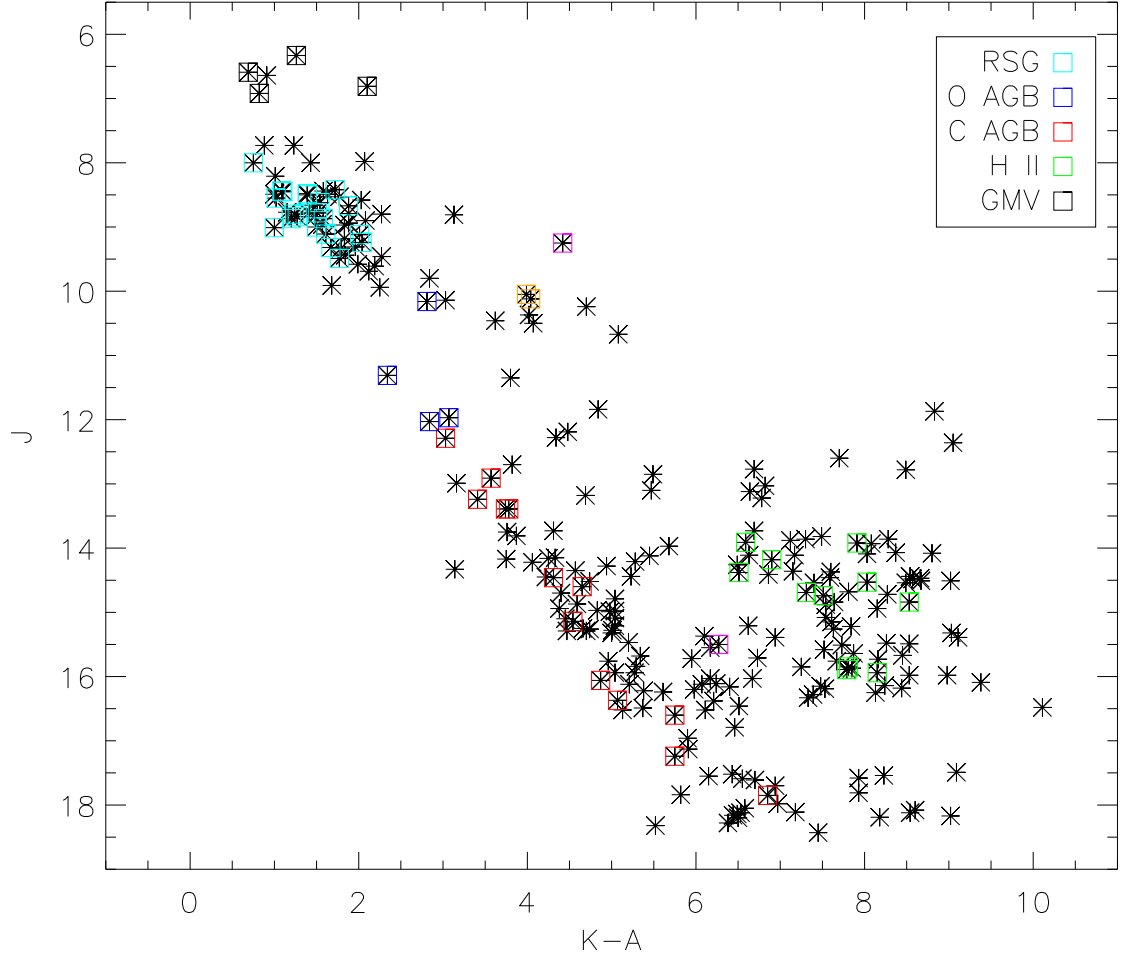


Fig. 3.— (a)  $2MASS/MSX J$  vs.  $K-A$  color-magnitude diagram for the Table 1 sample. The symbols are the same as Figure 2.

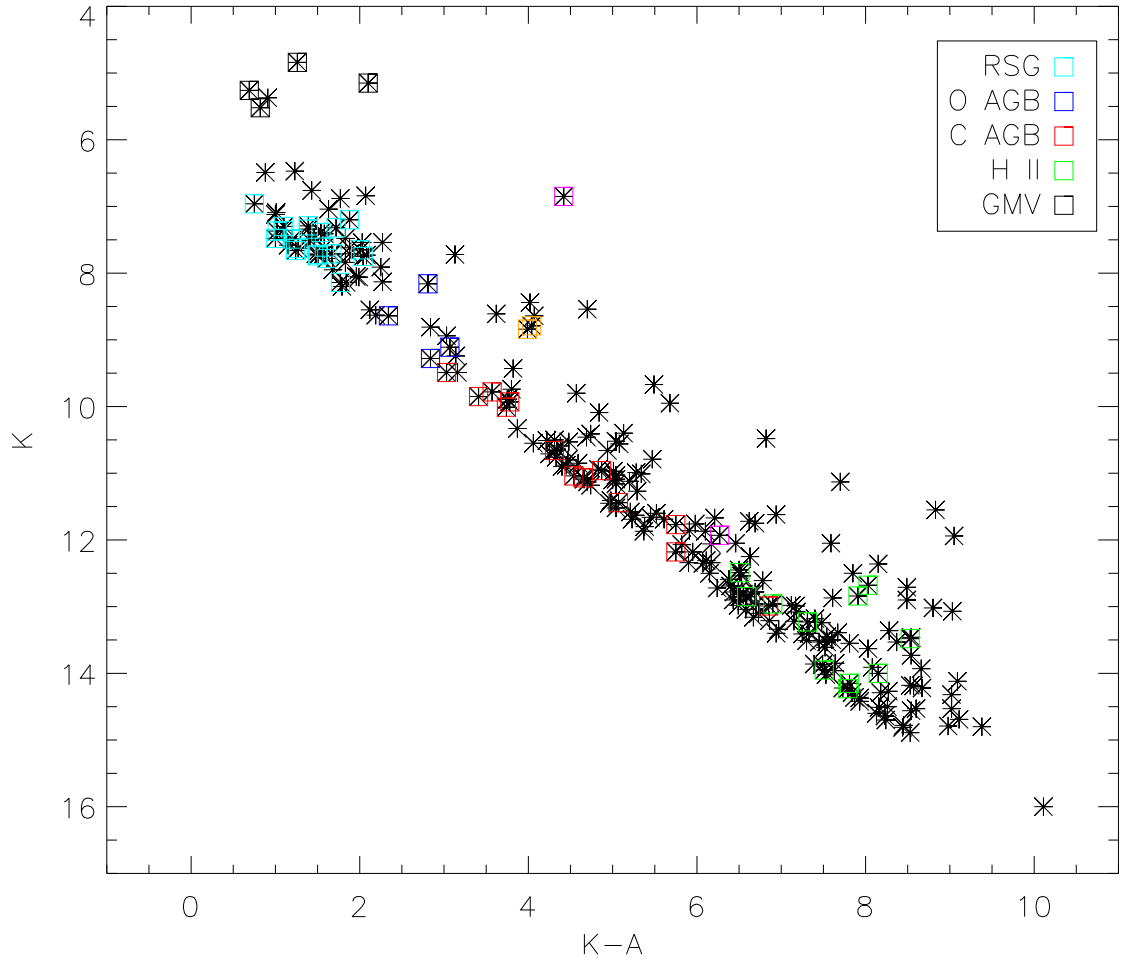


Fig. 3.— (b) As in Fig. 3 (a), but for  $K$  vs.  $K - A$ .

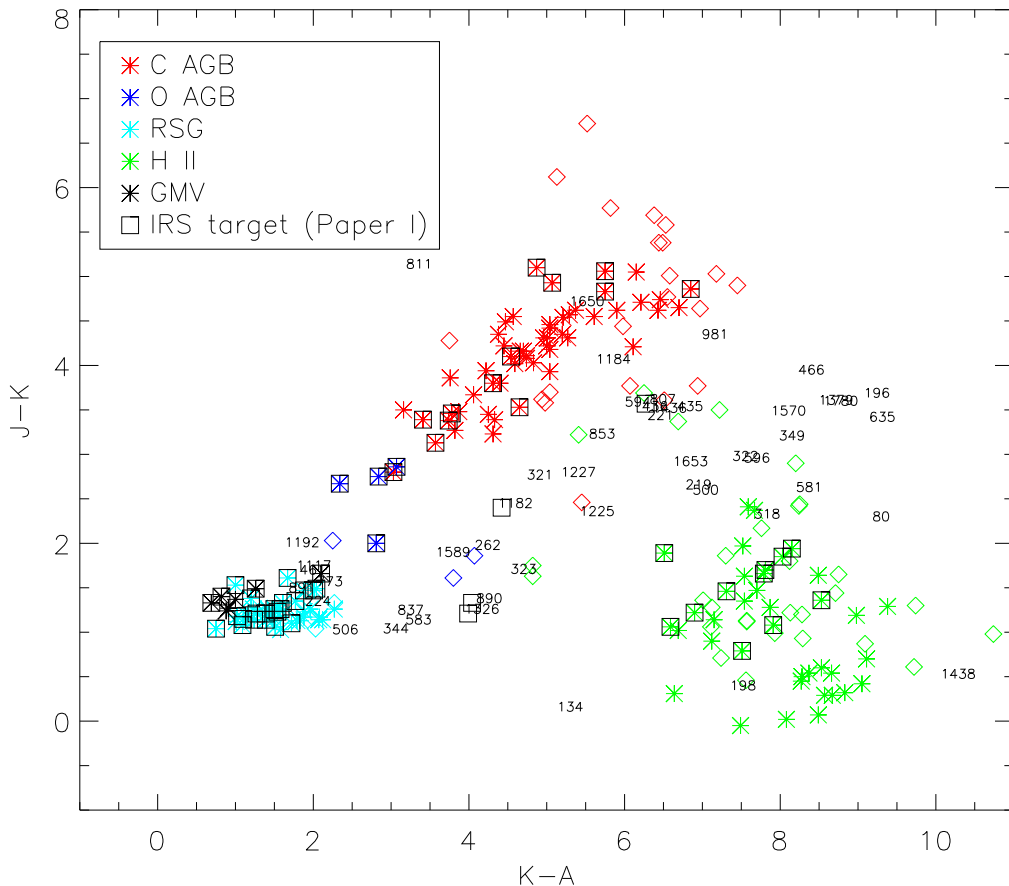


Fig. 4.— (a)  $J - K$  vs.  $K - A$  color-color diagram for the Table 1 sample, color-coded to illustrate the results of classification based on the *2MASS/MSX* color-color and color-magnitude diagrams (§3). Objects classified with high confidence are indicated by asterisks; objects with tentative classifications are indicated by diamonds. Points corresponding to objects included in the Paper I IRS sample are enclosed with small squares. Objects with no classification (or ambiguous/conflicting classifications) in Table 1 are indicated by MSX number.

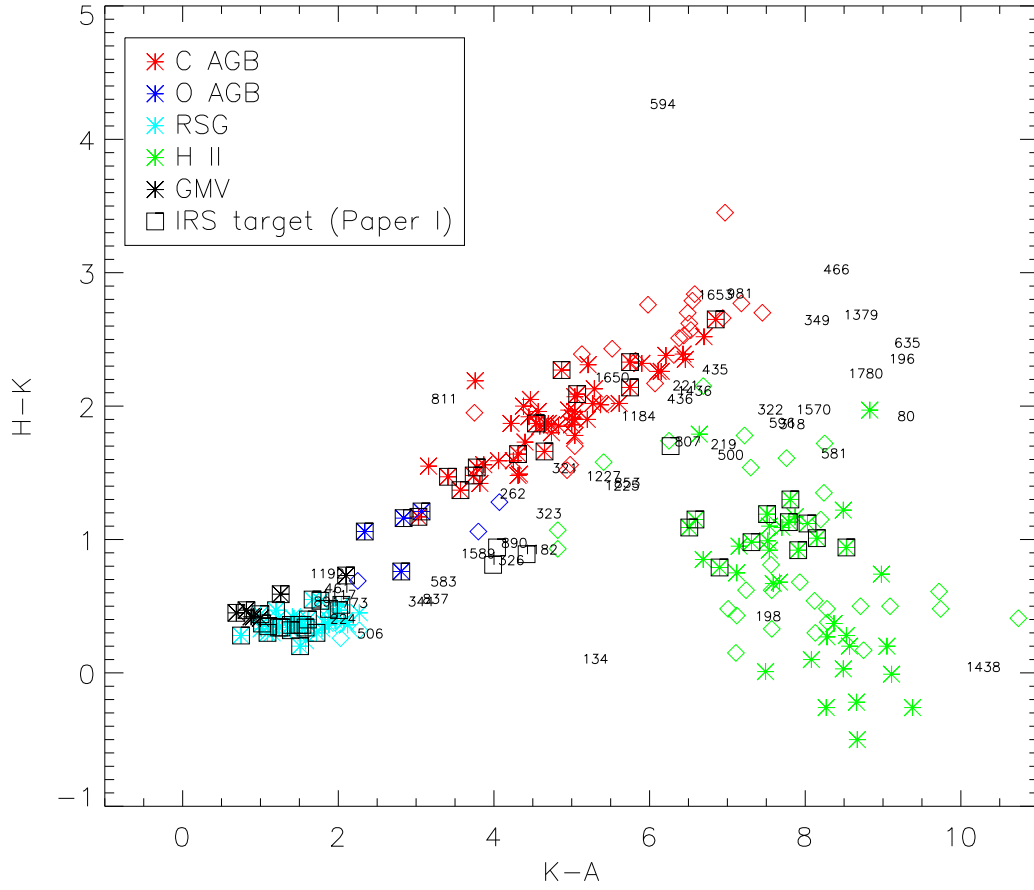


Fig. 4.— (b) As in Fig. 4 (a), but for  $H - K$  vs.  $K - A$  colors.

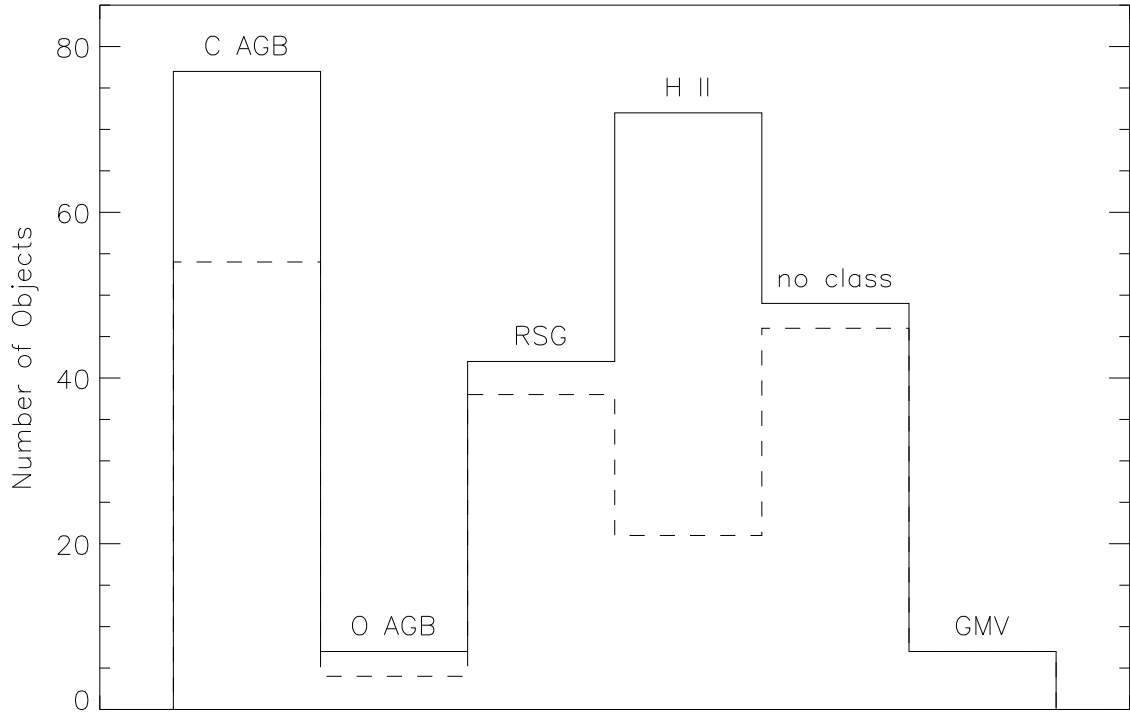


Fig. 5.— Histogram illustrating the number of objects in each *2MASS/MSX* infrared class. The (lower) dashed line indicates the number of objects classified with high confidence; the (upper) solid line indicates the total number of objects in each class when tentative classifications are included. The “no class” entry includes objects without *2MASS/MSX* classifications and objects with ambiguous and/or conflicting *2MASS/MSX* classifications.

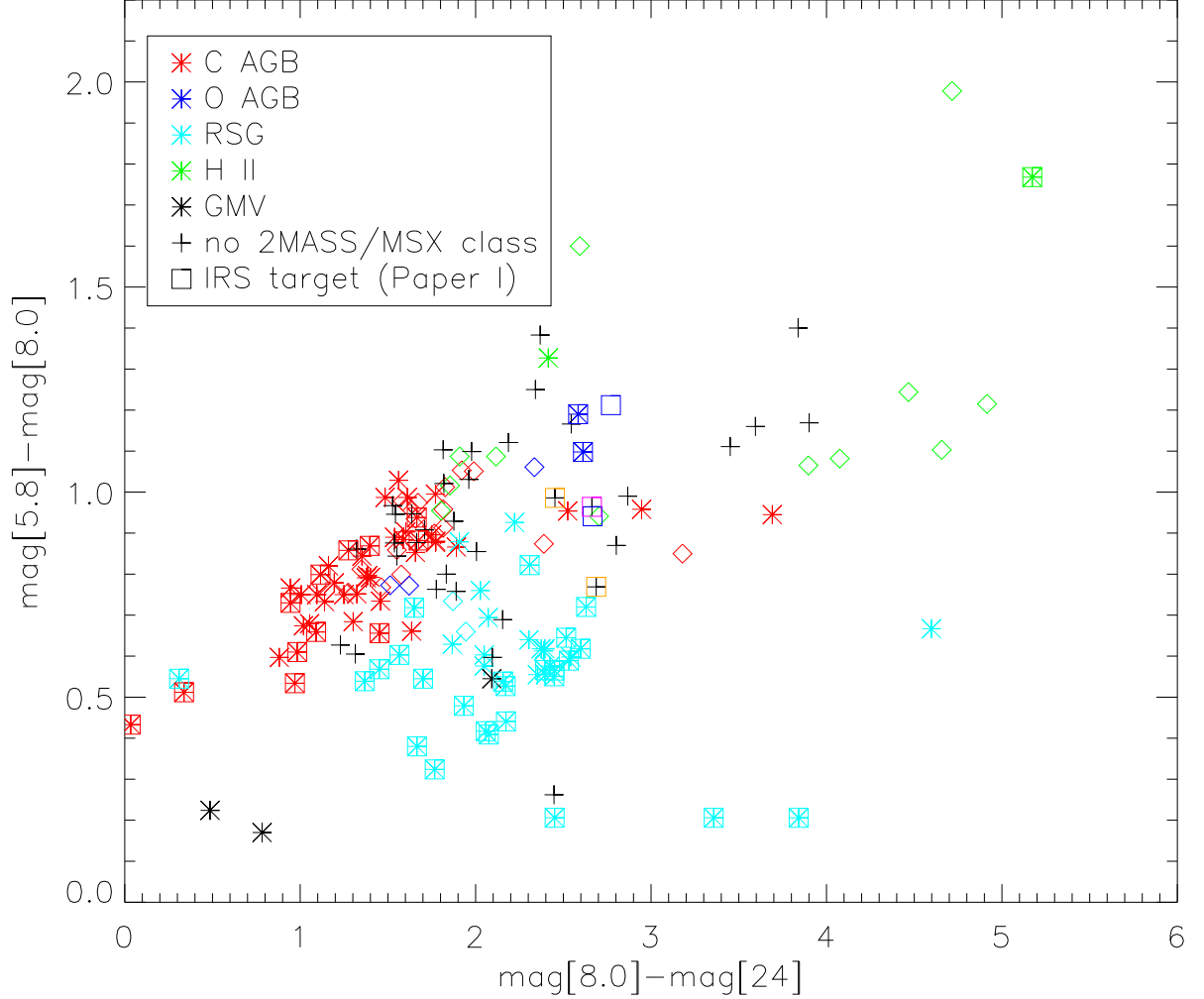


Fig. 6.— *Spitzer*  $[5.8] - [8.0]$  vs.  $[8.0] - [24]$  color-color diagram for the IRAC/MIPS counterparts to 172 Table 1 objects, constructed from SAGE point source catalog magnitudes. Symbol colors are as in Fig. 2. C-rich AGB stars and red supergiants appear as distinct clusters in the diagram (the three red supergiants near the bottom of the plot evidently have unreliable IRAC fluxes, perhaps as a result of detector saturation), as do IRS-confirmed O-rich AGB stars. The apparent paucity of H II regions is most likely a consequence of their spatial resolution by IRAC and consequent rejection from the SAGE/IRAC point source catalog.

Table 1. Objects in the A-band flux-limited *2MASS/MSX* Sample

LMC MSX number	SIMBAD name <sup>a</sup>	SIMBAD type <sup>a</sup>	J mag.	H mag.	K mag.	A mag.	EVP01	Classification Paper I	this paper <sup>b</sup>	L <sub>IR</sub> <sup>c</sup> L <sub>⊙</sub>
7	IRAS 05095-6525	IR	8.84	8.07	7.71	6.23	RSG		RSG	$8.0 \times 10^4$
21	IRAS 05053-6659	IR	15.58	14.60	13.61	6.09	PN		HII	
22	IRAS 05047-6644	IR	14.18	13.75	12.96	6.06	PN	HII	HII	$(6.8 \times 10^4)$
43	HV 888	M4Ia V*	8.00	7.17	6.76	5.33	O AGB		RSG	$1.9 \times 10^5$
44	IRAS 05112-6755	*	16.38	14.05	11.67	5.46	OH/IR		C AGB	$2.2 \times 10^4$
45	IRAS 05108-6839	IR	16.20	14.52	11.76	5.78	OH/IR		C AGB:	$1.6 \times 10^4$
46	LHA 120-N 17A	EmO	16.03	14.08	12.34	6.17	OH/IR		[HII]	
47			17.55	14.76	12.50	6.35	OH/IR		C AGB	$9.7 \times 10^3$
48			18.16	15.31	12.78	6.34	OH/IR		C AGB:	$9.7 \times 10^3$
80	EQ 051005.7-685634		15.32	14.96	13.07	4.04				
83	IRAS 05091-6904	IR	14.98	12.48	10.52	5.48	OH/IR		C AGB	$2.2 \times 10^4$
87			14.60	12.73	11.07	6.42	OH/IR	C AGB	C AGB	$9.3 \times 10^3$ ( $1.1 \times 10^4$ )
91	LI-LMC 372	IR	16.46	15.47	12.85	6.34	OH/IR		C AGB:	$9.7 \times 10^3$
95			13.39	11.49	10.01	6.27	C IR	C AGB	C AGB	$1.4 \times 10^4$ ( $1.4 \times 10^4$ )
108	IRAS 05113-6939	IR	15.28	12.88	10.97	5.96	OH/IR		C AGB	$1.4 \times 10^4$
134	HD 269006	?p Em*	10.67	10.63	10.56	5.48	HII			
138			15.84	13.40	11.27	5.98	OH/IR		C AGB	$1.4 \times 10^4$
141	WOH S 156	M *	8.84	7.97	7.63	6.36	RSG	RSG	RSG	$8.6 \times 10^4$ ( $9.2 \times 10^4$ )
196	IRAS 05125-7035	IR	18.17	16.85	14.53	5.51	OH/IR			
198	HD 269211	N *	13.86	13.90	13.51	6.21	HII		HII* <sup>d</sup>	
202			18.05	15.88	13.04	6.46	OH/IR		C AGB:	$8.6 \times 10^3$
215	LHA 120-N 113A	EmO	14.54	14.12	12.90	4.41	PN		HII	
216			11.35	10.80	9.74	5.94	PN		O AGB:	
217	IRAS 05137-6914	IR	14.69	14.21	13.23	5.92	PN	HII	HII	$(8.1 \times 10^4)$
218			13.39	11.47	9.93	6.15	OH/IR	C AGB	C AGB	$1.4 \times 10^4$ ( $1.3 \times 10^4$ )
219			15.71	14.78	13.10	6.37				
220			12.91	11.15	9.78	6.21	C IR	C AGB	C AGB	$1.6 \times 10^4$ ( $1.6 \times 10^4$ )
221			16.11	14.84	12.72	6.48	OH/IR			
222			14.74	15.14	13.95	6.44	PN	HII	HII	$(3.8 \times 10^4)$



Table 1—Continued

LMC MSX number	SIMBAD name <sup>a</sup>	SIMBAD type <sup>a</sup>	J mag.	H mag.	K mag.	A mag.	EVP01	Classification Paper I	this paper <sup>b</sup>	L <sub>IR</sub> <sup>c</sup> L <sub>⊙</sub>
223	LI-LMC 623	IR	17.84	14.41	12.07	6.25	OH/IR		C AGB:	$1.1 \times 10^4$
224	HD 269227	WN WR*	9.44	8.51	8.14	6.30			RSG <sup>d</sup>	$5.4 \times 10^4$
225			17.98	16.79	13.34	6.37	OH/IR		C AGB:	
262	HD 34664	B0Iab:e Em*	10.37	9.75	8.44	4.42	PN		C AGB: <sup>d</sup>	$6.7 \times 10^4$
263	HV 2360	M2Ia V*	8.90	8.12	7.73	5.65			RSG	$7.9 \times 10^4$
264	HV 916	M3Iab: V*	8.62	7.75	7.39	5.85	RSG	RSG	RSG	$1.1 \times 10^5$ ( $1.1 \times 10^5$ )
283	IRAS 05128-6455	*	13.73	11.98	10.50	6.19			C AGB	$1.2 \times 10^4$
307	IRAS 05190-6748	*	17.59	15.61	12.82	6.27	OH/IR		C AGB:	$1.0 \times 10^4$
318	IRAS 05195-6911	IR	15.15	14.70	12.87	5.26				
320	LI-LMC 810	IR	15.98	14.72	14.18	5.65	HII		HII:	
321	AGPRS J051904.02-	V*	13.18	11.96	10.46	5.77				
322			16.33	15.34	13.40	6.07				
323	ARDB 184	A0:Iab: Em*	12.19	11.69	10.53	6.05	PN			
325			15.25	12.96	11.09	6.43	OH/IR		C AGB	$9.2 \times 10^3$
341			17.52	15.29	12.90	6.47	OH/IR		C AGB	$8.6 \times 10^3$
344	HD 35231	?... V*	9.80	9.31	8.81	5.97				
349			17.58	17.03	14.42	6.49	OH/IR			
356			15.39	14.68	14.69	5.58	HII		HII*	
357			14.28	12.18	10.66	5.72	OH/IR		C AGB:	$1.7 \times 10^4$
358	[BE74] 560	Em*	15.98	15.53	14.79	5.81	HII		HII	
359	LHA 120-N 117	EmO	14.37	14.00	13.50	5.90	HII		HII:	
360	IRAS 05197-6950	IR	13.88	13.73	12.98	5.86	HII		HII	
362	ZZ Men	M3 sr*	8.49	7.53	7.12	6.12	O AGB		GMV	
398	IRAS 05182-7117	IR	14.84	14.53	13.85	6.21	HII		HII:	
412	RS Men	Me Mi*	6.59	5.71	5.26	4.57	O AGB	GMV	GMV	$(6.0 \times 10^3)$
420			14.94	12.59	10.59	6.21	OH/IR		C AGB	$1.2 \times 10^4$
435	LI-LMC 986	IR	15.21	13.96	11.72	5.10	OH/IR			
436			15.55	14.08	12.06	5.89	OH/IR			

Table 1—Continued

LMC MSX number	SIMBAD name <sup>a</sup>	SIMBAD type <sup>a</sup>	J mag.	H mag.	K mag.	A mag.	EVP01	Classification Paper I	this paper <sup>b</sup>	L <sub>IR</sub> <sup>c</sup> L <sub>⊙</sub>
438	LI-LMC 1028	IR	16.06	13.23	10.96	6.09	OH/IR	C AGB	C AGB	$1.2 \times 10^4$ ( $1.1 \times 10^4$ )
441			17.54	15.79	14.64	6.41			HII:	
461	LHA 120-N 132E	EmO	8.53	7.48	6.88	5.11	O AGB		GMV / RSG <sup>d</sup>	
464	[HS66] 272	OpC	14.21	12.57	10.99	5.71	OH/IR		[HII]	
465	IRAS 05253-6830	IR	13.93	14.01	13.91	5.83	HII		HII*	
466			18.19	17.28	14.29	6.11	OH/IR			
467			15.48	14.60	14.50	6.24	HII		HII:	
468	BSDL 1469	As*	15.51	14.38	14.22	6.49	HII		HII:	
469			15.67	14.90	14.78	6.33	HII		HII:	
470	NGC 1958	Cl*	13.73	13.05	12.78	6.09	HII		HII:	
500	LI-LMC 861	*	13.03	12.08	10.48	3.66				
501	NGC 1936	?e... EmO	15.87	14.65	12.50	4.65	OH/IR		[HII]	
502	IRAS 05230-6807	IR	14.51	14.41	14.32	5.30	HII		HII*	
503			14.88	14.45	13.53	5.99	PN		HII	
505			16.18	15.12	14.81	6.37	HII		HII:	
506	BSDL 1474	Neb	9.61	8.89	8.63	6.44				
507			14.26	13.41	12.98	6.49	HII		HII:	
522			13.12	14.60	12.81	6.17	PN		HII*	
529	HV 12793	M3/M4 V*	9.00	8.10	7.74	6.24	RSG	RSG	RSG	$7.8 \times 10^4$ ( $7.9 \times 10^4$ )
549	NGC 1948 WBT 54	*iC	9.32	8.26	7.71	6.04	O AGB	RSG	RSG	$8.0 \times 10^4$ ( $7.9 \times 10^4$ )
551	GRRV 43	M4 V*	9.33	8.53	8.20	6.41			RSG	$5.1 \times 10^4$
558	HV 2595	M1 Ia V*	8.58	7.80	7.54	5.51			RSG:	$9.4 \times 10^4$
559	[HCB95] LH 52 4978	UV	14.38	13.58	12.49	5.98	PN	HII	HII	$(2.0 \times 10^5)$
560	IRAS 05300-6651	*	18.12	15.11	12.54	6.01	OH/IR		C AGB:	$1.3 \times 10^4$
561	IRAS 05293-6715	PN	14.17	11.84	9.89	6.14	OH/IR		C AGB:	$1.5 \times 10^4$
562	KMHK 915	Cl*	12.28	11.72	10.65	6.31	PN		[HII]	
563	NGC 1974	Cl*	13.82	13.88	13.87	6.38	HII		HII*	
581			14.94	13.97	12.36	4.21				

Table 1—Continued

LMC MSX number	SIMBAD name <sup>a</sup>	SIMBAD type <sup>a</sup>	J mag.	H mag.	K mag.	A mag.	EVP01	Classification Paper I	this paper <sup>b</sup>	L <sub>IR</sub> <sup>c</sup> L <sub>⊙</sub>
582	[BE74] 292	Em*	12.78	12.74	12.71	4.22	HII		HII*	
583	HD 269599	Em*	8.81	8.37	7.72	4.59			[HII] <sup>d</sup>	
585	HD 269551	B Em*	7.98	7.22	6.84	4.77			RSG <sup>d</sup>	$1.8 \times 10^5$
587			9.12	8.12	7.65	5.64	O AGB	RSG	RSG	$8.4 \times 10^4$ ( $8.5 \times 10^4$ )
588	IRAS 05281-6915	M1 *	8.94	8.07	7.71	5.83			RSG	$8.0 \times 10^4$
589	SP77 46-19	M2Iab;+. *	8.50	7.65	7.29	5.90	RSG	RSG	RSG	$1.2 \times 10^5$ ( $1.3 \times 10^5$ )
590	BSDL 1943	As*	8.44	7.65	7.41	5.83	RSG		RSG	$1.1 \times 10^5$
591	IRAS 05313-6913	IR	9.46	8.45	8.13	5.86			RSG:	$5.4 \times 10^4$
592	HV 2532	M4 V*	8.96	8.06	7.71	6.14	RSG		RSG	$8.0 \times 10^4$
593	HV 2561	M0Ia V*	8.48	7.66	7.34	5.95	RSG	RSG	RSG	$1.1 \times 10^5$ ( $1.2 \times 10^5$ )
594			15.72	16.41	12.18	6.23	OH/IR			
596	IRAS 05311-6836	IR	16.15	15.08	13.24	5.76				
597	IRAS 05300-6859	M1Ia *	8.00	7.24	6.96	6.21	RSG	RSG	RSG	$1.6 \times 10^5$ ( $1.6 \times 10^5$ )
598	HV 2604	M1 V*	8.77	7.88	7.58	6.43	RSG		RSG	$9.0 \times 10^4$
599			16.14	15.20	14.70	6.46	HII		HII:	
601			14.70	12.63	10.90	6.50	OH/IR		C AGB	$9.0 \times 10^3$
635	IRAS 05278-6942	IR	17.49	16.56	14.12	5.03	OH/IR			
638	IRAS 05320-7106	IR	14.54	13.66	13.18	5.78	HII		HII:	
639			14.68	13.88	13.55	5.74	HII		HII:	
640	LHA 120-N 129	EmO	14.72	14.01	14.27	6.00	HII		HII*	
642	IRAS 05294-7104	*	11.31	9.70	8.64	6.30	C IR	O AGB	O AGB	$(4.2 \times 10^4)$
643			14.12	13.68	11.66	6.21			C AGB:	$1.1 \times 10^4$
644			16.12	13.89	11.58	6.37	OH/IR		C AGB	$9.5 \times 10^3$
645			13.81	11.89	10.33	6.46	OH/IR		C AGB	$1.1 \times 10^4$
646	[MLD95] LMC 1- 289	O7.5Ve *	15.73	14.81	14.51	6.35	HII		HII:	
651	IRAS 05310-7110	IR	15.26	14.44	13.96	6.33	HII		HII:	
653	IRAS 05298-6957	*	13.75	12.08	9.89	6.13	OH/IR		C AGB	$1.5 \times 10^4$ :
661			15.76	13.42	11.45	6.49	OH/IR		C AGB	$8.5 \times 10^3$
689			15.29	12.85	10.80	6.33	OH/IR		C AGB	$1.0 \times 10^4$

Table 1—Continued

LMC MSX number	SIMBAD name <sup>a</sup>	SIMBAD type <sup>a</sup>	J mag.	H mag.	K mag.	A mag.	EVP01	Classification Paper I	this paper <sup>b</sup>	L <sub>IR</sub> <sup>c</sup> L <sub>⊙</sub>
690			15.22	14.67	14.29	6.45	HII		HII:	
692			16.49	13.88	11.87	6.50	OH/IR		C AGB	$8.4 \times 10^3$
716	HV 12830	M V*	6.64	5.79	5.37	4.46	O AGB		GMV	
720			15.94	13.59	11.52	6.48	OH/IR		C AGB	$8.6 \times 10^3$
733	IRAS 05348-7024	*	16.79	14.40	12.05	5.59	OH/IR		C AGB	$1.9 \times 10^4$
745			14.99	12.97	11.41	6.43	OH/IR		C AGB:	$9.0 \times 10^3$
764	IRAS 05333-6948	IR	13.92	13.76	12.84	4.93	PN	HII	HII	$(2.7 \times 10^5)$
766	LHA 120-N 150	HII	14.47	13.71	13.93	5.27	HII		HII*	
767	IRAS 05363-6940	IR	14.48	14.39	14.19	5.62	HII		HII*	
768			15.21	12.93	11.03	5.99	OH/IR		C AGB	$1.4 \times 10^4$
769			15.08	14.55	13.45	5.91	PN		HII	
770	MDM 49	Rad	14.36	14.17	13.22	6.07	PN		HII	
771			16.52	14.57	12.31	6.20	OH/IR		C AGB	$1.1 \times 10^4$
772			14.41	13.69	13.21	6.35	HII		HII:	
773	BAT99 69	WC WR*	9.58	8.55	8.06	6.07	O AGB		GMV / RSG <sup>d</sup>	
774			17.61	15.48	12.96	6.26	OH/IR		C AGB	$1.0 \times 10^4$
775			13.24	11.32	9.85	6.44	C IR	C AGB	C AGB	$1.3 \times 10^4$ ( $1.9 \times 10^4$ )
804	IRAS 05325-6743	IR	14.07	13.90	13.53	5.16	HII		HII*	
805	LI-LMC 1163	M1Ia *	8.80	7.99	7.54	5.27			RSG	$9.4 \times 10^4$
806	LHA 120-N 57E	EmO	11.84	11.02	10.09	5.25	PN		[HII]	
807			15.50	13.63	11.93	5.66	OH/IR	OH/IR		$(4.0 \times 10^4)$
809	HV 5933	M4Iab: V*	8.97	8.21	7.84	6.01			RSG	$7.1 \times 10^4$
810	CCDM J05303-6653B	*i*	8.78	7.92	7.72	6.21	RSG	RSG	RSG	$7.9 \times 10^4$ ( $9.4 \times 10^4$ )
811			14.33	11.26	9.24	6.10				
813	HV 12437	M0.5 V*	9.69	8.91	8.55	6.43			RSG	$3.7 \times 10^4$
815	HV 1001	M4 V*	9.49	8.68	8.14	6.37	O AGB	RSG	RSG	$5.4 \times 10^4$ ( $5.5 \times 10^4$ )
836	IRAS 05325-6629	IR	15.94	15.01	14.00	5.85	PN	HII	HII	$(7.7 \times 10^4)$
837			10.14	9.46	8.94	5.91				

Table 1—Continued

LMC MSX number	SIMBAD name <sup>a</sup>	SIMBAD type <sup>a</sup>	J mag.	H mag.	K mag.	A mag.	EVP01	Classification Paper I	this paper <sup>b</sup>	L <sub>IR</sub> <sup>c</sup> L <sub>⊙</sub>
839			8.44	7.66	7.36	6.27	RSG	RSG	RSG	$1.1 \times 10^5$ ( $1.2 \times 10^5$ )
840	IRAS 05297-6517	IR	15.09	12.94	11.16	6.12	OH/IR		C AGB	$1.2 \times 10^4$
853	IRAS 05307-6410	IR	12.85	11.06	9.67	4.18				
869			8.66	7.87	7.48	6.02	RSG		RSG	$9.9 \times 10^4$
870	Dachs LMC 2-16	M3Iab: *	8.45	7.65	7.30	6.20	RSG	RSG	RSG	$1.2 \times 10^5$
885	[P93] 1339	B0IV *	11.87	13.52	11.55	2.72	PN		HII*	
886	IRAS 05389-6922	M0.5 IR	10.24	9.40	8.54	3.84	PN		[RSG]	
887	IRAS 05406-6924	IR	10.50	9.92	8.64	4.57	PN		O AGB:	
888			15.39	14.28	11.62	4.68	OH/IR		C AGB:	$4.4 \times 10^4$
889	[JGB98] 30 Dor-06	MoC	14.53	13.80	12.68	4.65	PN	HII	HII	$(4.0 \times 10^5)$
890	HD 37974	B:e Em*	10.12	9.73	8.79	4.75	PN	Peculiar		$(7.1 \times 10^4)$
891			8.49	7.54	7.04	5.41	O AGB		GMV / RSG	
892	BRHT 54b	Cl*	8.79	8.02	7.62	5.74			RSG	$8.7 \times 10^4$
893	IRAS 05413-6919	IR	8.78	7.93	7.51	6.10	O AGB		RSG	$9.6 \times 10^4$
894	LHA 120-N 158B	EmO	13.91	14.00	12.85	6.26	PN	HII	HII	$(5.6 \times 10^4)$
897			8.87	7.96	7.49	6.29	O AGB	RSG	RSG	$6.3 \times 10^4$ ( $9.4 \times 10^4$ )
900	[P93] 1938	O7.5Vb: *	15.64	15.53	14.36	6.49	PN		HII	
906			16.28	15.21	13.86	6.47			HII:	
930	[DMM94] J0539-696	Rad	12.36	12.14	11.94	2.89	HII		HII*	
932	IRAS 05405-6946	IR	14.08	13.17	13.02	4.22	HII		HII:	
934	[JGB98] N158-2	MoC	14.84	14.42	13.48	4.95	PN	HII	HII	$(2.5 \times 10^5)$
936	IRAS 05402-6956	*	14.35	11.76	9.80	5.23	OH/IR		C AGB	$2.8 \times 10^4$
937	IRAS 05410-6954	IR	14.52	12.27	10.41	5.67	OH/IR		C AGB	$1.8 \times 10^4$
938	IRAS 05389-7042	IR	14.09	14.44	13.63	5.60	PN		HII:	
939	[HS66] 385	OpC	9.24	8.26	7.75	5.71	O AGB	RSG	RSG	$7.7 \times 10^4$ ( $8.1 \times 10^4$ )
940	[KRB97] 30DorCent	MoC	15.85	15.13	13.41	6.16			[HII]	
941			15.10	12.80	10.88	6.43	OH/IR		C AGB	$9.5 \times 10^3$
942	BSDL 2601	As*	16.25	14.77	14.60	6.47	HII		HII:	

Table 1—Continued

LMC MSX number	SIMBAD name <sup>a</sup>	SIMBAD type <sup>a</sup>	J mag.	H mag.	K mag.	A mag.	EVP01	Classification Paper I	this paper <sup>b</sup>	L <sub>IR</sub> <sup>c</sup> L <sub>⊙</sub>
943	HV 2778	M0 V*	8.80	8.00	7.66	6.42	RSG	RSG	RSG	$8.4 \times 10^4$ ( $8.7 \times 10^4$ )
977	IRAS 05406-7111	IR	16.09	14.54	14.80	5.42	HII		HII*	
978	[O96] D293 - 39	*	15.76	14.07	13.39	5.72			HII*	
981			17.70	16.21	13.40	6.46	OH/IR			
1016			16.22	13.72	11.80	6.42	OH/IR		C AGB	$9.0 \times 10^3$
1048	RT Men	Mi*	7.73	6.91	6.49	5.61	O AGB		GMV	
1072	IRAS 04407-7000	*	10.16	8.92	8.16	5.35	PN	O AGB	O AGB	$(6.5 \times 10^4)$
1107	[FHW95] LMC B0452-	1 HII	14.46	12.72	12.05	4.46			HII*	
1115	IRAS 04496-6917	IR	13.86	13.63	13.36	5.08	HII		HII*	
1117	IRAS 04498-6842	*	9.18	8.03	7.48	5.65	O AGB		GMV / RSG	
1119			14.22	12.14	10.55	6.49	OH/IR		C AGB	$9.9 \times 10^3$
1120	LI-LMC 31	IR	14.46	12.30	10.66	6.35	OH/IR	C AGB	C AGB	$1.1 \times 10^4$ ( $1.1 \times 10^4$ )
1130	IRAS 04496-6958	C*	12.70	10.85	9.43	5.61			C AGB	$2.4 \times 10^4$
1132	HV 2236	M V*	9.11	8.18	7.78	6.17	O AGB	RSG	RSG	$7.5 \times 10^4$ ( $7.7 \times 10^4$ )
1150	WOH G 17	*	6.92	5.99	5.52	4.70	O AGB	GMV	GMV	$(4.0 \times 10^3)$
1171	IRAS 04545-7000	*	16.52	12.79	10.40	5.27	OH/IR		C AGB:	$2.6 \times 10^4$
1173	IRAS 04523-7043	IR	18.32	14.03	11.60	6.08	OH/IR		C AGB:	$1.2 \times 10^4$
1182	IRAS 04553-6825	M7.5 *	9.25	7.74	6.85	2.43		OH/IR		$(4.7 \times 10^5)$
1183	BSDL 126	Neb	12.60	12.22	11.13	3.43	PN		HII	
1184	IRAS 04530-6916	*	13.97	11.84	9.95	4.27	OH/IR		C AGB: <sup>e</sup>	
1186	IRAS 04542-6916	IR	14.44	13.87	13.46	4.92	HII		HII:	
1187	[L72] LH 5-1008	*iA	12.77	12.60	11.75	5.06	PN		HII	
1189	IRAS 04553-6933	M2 IR	8.67	7.68	7.20	5.32	O AGB	RSG	RSG	$1.3 \times 10^5$ ( $1.3 \times 10^5$ )
1190	IRAS 04516-6902	*	9.94	8.60	7.91	5.66			O AGB:	
1191	WOH S 60	M *	9.31	8.44	8.05	6.09			RSG	$5.9 \times 10^4$
1192	IRAS 04509-6922	*	9.91	8.66	7.95	6.27			GMV / O AGB	
1193			15.29	13.00	11.13	6.43	OH/IR		C AGB	$9.2 \times 10^3$
1204	SP77 31-18	M *	8.55	7.74	7.37	6.35	RSG	RSG	RSG	$1.1 \times 10^5$ ( $1.0 \times 10^5$ )
1207	LHA 120-N 89	EmO	15.37	13.65	11.87	5.77	OH/IR		[HII]	

Table 1—Continued

LMC MSX number	SIMBAD name <sup>a</sup>	SIMBAD type <sup>a</sup>	J mag.	H mag.	K mag.	A mag.	EVP01	Classification Paper I	this paper <sup>b</sup>	L <sub>IR</sub> <sup>c</sup> L <sub>⊙</sub>
1225			13.10	12.16	10.79	5.32				
1227			14.44	13.13	11.69	6.46				
1229			16.19	15.63	14.02	6.49			HII:	
1247	PGMW 3123	O8.5V *	14.44	14.35	13.73	5.19	HII		HII:	
1248	PGMW 3265	*	13.22	13.22	12.61	5.83	HII		HII:	
1249			14.15	12.25	10.76	6.43			C AGB	$9.7 \times 10^3$
1278	IRAS 05009-6616	*	16.12	14.52	12.35	6.28	OH/IR		C AGB:	$1.0 \times 10^4$
1280	IRAS 05003-6712	*	12.03	10.44	9.28	6.44	C IR	O AGB	O AGB	$(1.7 \times 10^4)$
1282			17.24	14.51	12.18	6.43	OH/IR	C AGB	C AGB	$9.0 \times 10^3$ ( $1.5 \times 10^4$ )
1296	HD 32364	?e *	14.11	13.79	12.25	5.62	PN		HII:	
1297	IRAS 04573-6849	IR	14.51	13.72	14.22	5.55	HII		HII*	
1298			15.47	13.02	11.12	5.92	OH/IR		C AGB	$1.4 \times 10^4$
1302	IRAS 04589-6825	IR	15.49	15.17	14.89	6.36	HII		HII*	
1306	LHA 120-S 5	EmO	15.85	15.45	14.15	6.34	PN	HII	HII	$(4.3 \times 10^4)$
1326	HD 268835	B8Ia Em*	10.05	9.65	8.84	4.85	PN	Peculiar		$(5.5 \times 10^4)$
1328	HV 2255	M4 V*	8.42	7.62	7.32	5.60	RSG	RSG	RSG	$1.1 \times 10^5$ ( $1.3 \times 10^5$ )
1329	WOH S 76	M *	8.21	7.42	7.09	6.08	RSG		RSG	$1.4 \times 10^5$
1330	WOH S 74	M *	8.87	7.95	7.61	6.03	RSG	RSG	RSG	$8.8 \times 10^4$ ( $9.3 \times 10^4$ )
1360			18.14	15.46	12.76	6.27	OH/IR		C AGB:	$1.0 \times 10^4$
1371	IRAS 05469-7255	IR	14.79	12.79	11.09	6.05	OH/IR		C AGB:	$1.3 \times 10^4$
1378			16.24	13.71	11.69	6.08	OH/IR		C AGB	$1.2 \times 10^4$
1379			18.12	17.21	14.56	6.02	OH/IR			
1382	PMN J0545-6946	Rad	14.11	13.61	12.99	5.82	HII		HII:	
1383	LI-LMC 1646	IR	18.11	15.85	13.08	5.90	OH/IR		C AGB:	$1.4 \times 10^4$
1384			16.37	13.53	11.44	6.37	OH/IR	C AGB	C AGB	$9.5 \times 10^3$ ( $5.8 \times 10^3$ )
1400			16.60	13.91	11.77	6.02	OH/IR	C AGB	C AGB	$1.3 \times 10^4$ ( $7.1 \times 10^3$ )
1411	IRAS 05410-6520	IR	17.13	14.67	11.86	5.95	OH/IR		C AGB:	
1412	IRAS 05404-6458	IR	15.32	12.96	11.10	6.10	OH/IR		C AGB	$1.2 \times 10^4$

Table 1—Continued

LMC MSX number	SIMBAD name <sup>a</sup>	SIMBAD type <sup>a</sup>	J mag.	H mag.	K mag.	A mag.	EVP01	Classification Paper I	this paper <sup>b</sup>	$L_{\text{IR}}^c$ $L_{\odot}$
1429	HV 2834	M0.5 V*	9.01	7.92	7.48	6.48	O AGB	RSG	RSG	$9.9 \times 10^4$ ( $9.1 \times 10^4$ )
1436			16.16	14.77	12.69	6.29	OH/IR			
1438	HD 269997	B3Ia *	16.48	16.01	16.00	5.89	HII		HII* <sup>d</sup>	
1453	IRAS 05506-7053	*	18.20	15.34	12.45	5.95	OH/IR		C AGB:	
1456			12.99	11.04	9.49	6.33			C AGB	$1.8 \times 10^4$
1471			16.96	14.66	12.34	6.44	OH/IR		C AGB	$8.9 \times 10^3$
1488	IRAS 05508-7146	IR	15.14	12.91	11.04	6.50	OH/IR	C AGB	C AGB	$8.8 \times 10^3$ ( $1.1 \times 10^4$ )
1492			12.29	10.66	9.49	6.46	C IR	C AGB	C AGB	( $1.9 \times 10^4$ )
1524	IRAS 05558-7000	*	11.97	10.32	9.11	6.04	C IR	O AGB	O AGB	( $4.1 \times 10^4$ )
1546			14.97	12.79	10.94	6.11	OH/IR		C AGB	$1.2 \times 10^4$
1567	IRAS 05526-6520	IR	15.94	13.65	11.63	6.36	OH/IR		C AGB	$9.6 \times 10^3$
1570	IRAS 05540-6533	IR	17.81	16.31	14.37	6.44	OH/IR			
1571	IRAS 05547-6515	IR	18.28	15.10	12.59	6.21	OH/IR		C AGB:	$1.1 \times 10^4$
1589	IRAS 05571-6827	IR	10.46	9.47	8.61	4.99	PN			
1650	IRAS 06024-6645A	B3 HV*	15.68	13.19	11.01	5.67	OH/IR		C AGB <sup>d</sup>	$1.8 \times 10^4$
1651			18.43	16.23	13.53	6.08	OH/IR		C AGB:	$1.2 \times 10^4$
1652	IRAS 06025-6712	IR	17.85	15.64	12.99	6.14	OH/IR	C AGB	C AGB	$1.1 \times 10^4$ ( $1.2 \times 10^4$ )
1653			16.03	15.96	13.16	6.49				
1677	IRAS 06013-6505	IR	6.81	5.88	5.15	3.05	O AGB	GMV	GMV	( $9.7 \times 10^3$ )
1679			7.73	6.88	6.47	5.24	O AGB		RSG	$2.5 \times 10^5$
1686			6.33	5.43	4.84	3.58	C AGB	GMV	GMV	( $4.6 \times 10^3$ )
1689			14.87	12.70	10.85	6.26	OH/IR		C AGB	$1.1 \times 10^4$
1696			14.45	12.38	10.51	6.29	OH/IR		C AGB	$1.1 \times 10^4$
1753			15.26	12.98	11.18	6.44	OH/IR		C AGB	$9.1 \times 10^3$
1780			18.08	16.74	14.53	5.93	OH/IR			
1794			15.89	15.36	14.23	6.44	PN	HII	HII	( $1.7 \times 10^4$ )
1797			14.16	12.30	10.71	6.46	OH/IR		C AGB	$9.6 \times 10^3$



<sup>a</sup>Source types and names from SIMBAD, [simbad.u-strasbg.fr/sim-fid.pl](http://simbad.u-strasbg.fr/sim-fid.pl). Spectral types are indicated where known, blank indicates that the object is of unknown object or spectral type. V\* indicates a variable star, EmO indicates emission object, IR indicates Infrared, \* indicates star, WN indicates Wolf-Rayet, sr\* indicates semi-regular pulsating star, Mi\* indicates variable star of mira cet type, OpC indicates open cluster, As\* indicates association of stars, Cl\* indicates cluster of stars, \*iC indicates star in cluster, \*i\* indicates star in double system, MoC indicates molecular cloud, Rad indicates radio source, \*iA indicates star in association, HV\* indicates high-velocity star.

<sup>b</sup>Source types with colons are those that appear in only one box in the color-color plots of figure 2. Source types with square brackets are classified based on their SIMBAD type and J, H, K, A colors. HII source types with asterisks are those that appear just below the HII classification box. Objects with that are unclassifiable on the basis of  $2MASS/MSX$  colors are left blank (see §3).

<sup>c</sup>L<sub>IR</sub> values within parenthesis are from Paper I.

<sup>d</sup>2MASS/MSX color classification conflicts with information in SIMBAD.

<sup>e</sup>Young stellar object; emission-line spectrum in infrared (van Loon et al. 2001, 2005).

Table 2. Summary of classifications of luminous 8  $\mu\text{m}$  sources in the LMC

Class	EVP01	Paper I	this paper <sup>a</sup>
All	254	57	254
H II	42	11	72 (51)
RSG	19	21	42 (4)
O AGB	21	4	7 (3)
C AGB	8 <sup>b</sup>	13	77 (23)
GMV	0	4	7
PN	34	0	0 <sup>c</sup>
OH/IR	88	2	... <sup>d</sup>
Peculiar	0	2	... <sup>d</sup>
Unclassified	50	0	36
Ambiguous	...	...	13 <sup>e</sup>

<sup>a</sup>Numbers in parentheses indicate number included that are tentative classifications. Numbers listed for H II, RSG, O AGB, and C AGB do not include objects for which *2MASS-MSX* and SIMBAD classifications are in conflict (see Table 1, footnote d) or objects for which *2MASS-MSX* color-color and/or color-magnitude classifications are ambiguous.

<sup>b</sup>Includes objects classified as either “C AGB” or “C IR”.

<sup>c</sup>A small fraction of objects classified as H II regions may be PNs; see §4.1.

<sup>d</sup>Classification criteria are not well defined.

<sup>e</sup>Objects with ambiguous *2MASS-MSX* classifications and objects for which *2MASS-MSX* and SIMBAD classifications are in conflict.

Table 3. 2MASS/MSX magnitude criteria for identifying object types.

Class	Magnitude criteria			
	J	H	K	A
[1]	[2]	[3]	[4]	[5]
GMV	$<7.5$	$\leq 7.5$	$\leq 6.0$	$<5.0$
RSG	$8.0 - 9.5$	$7.2 - 8.7$	$7.0 - 8.2$	$5.3 - 6.4$
O AGB	$10.2 - 12.0$	$8.9 - 10.3$	$8.2 - 9.1$	$5.3 - 6.3$
C AGB	$> [1.5(K-A)+5.5]$	$10.7 - 15.6$	$9.5 - 13.0$	$5.8 - 6.5$
H II	$< [1.5(K-A)+5.5]$	$13.6 - 15.4$	$12.5 - 14.2$	$4.7 - 6.4$

Note. — Columns: [1] Type of LMC or foreground object; [2]-[5] IR magnitude criteria.